1-1-2023

Structural gray matter alterations in glioblastoma and high-grade glioma- A potential biomarker of survival

Bidhan Lamichhane

Patrick H Luckett

Donna Dierker

Ki Yun Park

Harold Burton

See next page for additional authors

Authors

Bidhan Lamichhane, Patrick H Luckett, Donna Dierker, Ki Yun Park, Harold Burton, Michael Olufawo, Gabriel Trevino, John J Lee, Andy G S Daniel, Carl D Hacker, Daniel S Marcus, Joshua S Shimony, and Eric C Leuthardt

Neuro-Oncology Advances

5(1), 1–10, 2023 | https://doi.org/10.1093/noajnl/vdad034 | Advance Access date 14 April 2023

Structural gray matter alterations in glioblastoma and high-grade glioma—A potential biomarker of survival

Bidhan Lamichhane, Patrick H. Luckett, Donna Dierker, Ki Yun Park, Harold Burton, Michael Olufawo, Gabriel Trevino, John J. Lee, Andy G. S. Daniel, Carl D. Hacker, Daniel S. Marcus, Joshua S. Shimony, and Eric C. Leuthardt

[1]Department of Neurological Surgery, Washington University School of Medicine, St. Louis, Missouri, USA (B.L., P.H.L., K.Y.P., M.O., G.T., C.D.H., E.C.L); [2]Mallinckrodt Institute of Radiology, Washington University School of Medicine, St. Louis, Missouri, USA (D.D., J.J.L., D.S.M., J.S.S.); [3]Department of Neuroscience, Washington University School of Medicine, St. Louis, Missouri, USA (H.B., E.C.L.); [4]Department of Biomedical Engineering, Washington University in Saint Louis, St. Louis, Missouri, USA (A.G.S.D., E.C.L.); [5]Department of Mechanical Engineering and Materials Science, Washington University, St. Louis, Missouri, USA. (E.C.L.); [6]Center for Innovation in Neuroscience and Technology, Washington University School of Medicine, St. Louis, Missouri, USA (E.C.L.); [7]Brain Laser Center, Washington University School of Medicine, St. Louis, Missouri, USA (E.C.L.); [8]Division of Neurotechnology, Washington University School of Medicine, St. Louis, Missouri, USA (E.C.L.)

Corresponding Author: Bidhan Lamichhane, PhD, Department of Neurosurgery, Washington University School of Medicine, Box 8057, 660 South Euclid, St. Louis, MO 63110, USA (bidhanlamichhane@wustl.edu)

Abstract

Background. Patients with glioblastoma (GBM) and high-grade glioma (HGG, World Health Organization [WHO] grade IV glioma) have a poor prognosis. Consequently, there is an unmet clinical need for accessible and noninvasively acquired predictive biomarkers of overall survival in patients. This study evaluated morphological changes in the brain separated from the tumor invasion site (ie, contralateral hemisphere). Specifically, we examined the prognostic value of widespread alterations of cortical thickness (CT) in GBM/HGG patients.

Methods. We used FreeSurfer, applied with high-resolution T1-weighted MRI, to examine CT, evaluated prior to standard treatment with surgery and chemoradiation in patients (GBM/HGG, $N = 162$, mean age 61.3 years) and 127 healthy controls (HC; 61.9 years mean age). We then compared CT in patients to HC and studied patients' associated changes in CT as a potential biomarker of overall survival.

Results. Compared to HC cases, patients had thinner gray matter in the contralesional hemisphere at the time of tumor diagnosis. patients had significant cortical thinning in parietal, temporal, and occipital lobes. Fourteen cortical parcels showed reduced CT, whereas in 5, it was thicker in patients' cases. Notably, CT in the contralesional hemisphere, various lobes, and parcels was predictive of overall survival. A machine learning classification algorithm showed that CT could differentiate short- and long-term survival patients with an accuracy of 83.3%.

Conclusions. These findings identify previously unnoticed structural changes in the cortex located in the hemisphere contralateral to the primary tumor mass. Observed changes in CT may have prognostic value, which could influence care and treatment planning for individual patients.

Key Points

- Glioblastoma and high-grade glioma (GBM/HGG) patients demonstrated structural alterations in the hemisphere contralateral from the tumor.
- Brain morphometric changes were present at the time of tumor diagnosis.
- Cortical thickness (CT) may provide biomarkers for survival duration in GBM/HGG.
- Machine learning classifier distinguished short- from long-term survival using CT with an accuracy of 83.3%.

Importance of the Study

Patients with glioblastoma and high-grade glioma (GBM/HGG; World Health Organization grade IV glioma) have poor survival with current treatments. Thus, there is an urgent need to identify biomarkers that could guide clinical trial protocols and possibly improve pretreatment planning. Morphometric assessments of tumors and immediate adjacent areas have routinely used structural MRI. However, the existence and effects of distant structural changes from the tumor invasion site have been underexamined. We examined the morphometric changes of patients and their relationship with overall survival using high-resolution T1-weighted MRI upon initial diagnosis. We contrasted images to comparable MRIs from healthy controls. MRIs from GBM/HGG patients showed widespread cortical thinning in the contralateral hemisphere. Importantly, cortical thickness (CT) was predictive of overall survival. A machine learning classification algorithm found that CT could differentiate short- and long-term survival patients with an accuracy of 83.3%. These findings could provide critical prognostic information to inform care.

The prognosis of glioblastoma and high-grade glioma (GBM/HGG) is very poor, with median overall survival (OS; the time of diagnosis of GBM/HGG to death) ranging from 12 to 15 months.[1] An unmet clinical need is accessible, noninvasively acquired predictive biomarkers (eg, biomarker of survival). Currently, structural MRI scans routinely provide morphometric radiologic assessments of the tumor; however, brain morphology contralateral to the tumor site may provide a predictive biomarker of prognosis, enable clinical decisions of care, and potentially guide aggressiveness of treatment with impacts on quality of life. Unfortunately, little is known about the existence of such morphological changes in the brain separated from the tumor invasion site, and the clinical importance of which has been underexamined.

Prior studies reported associations between brain-morphological changes with cognitive and motor impairment in healthy aging, sex, hemisphere, and diseases.[2–5] Significantly, patients with GBM/HGG often present with neurologic and cognitive deficits before initiating any treatment.[6,7] Tumor tissue invasion and localized mass effects traditionally explain these deficits. However, cognitive performance was more severely affected in patients with HGG than those with low-grade gliomas), even after accounting for tumor volumes.[8,9] These findings suggested widespread disturbances in brain morphometry existed beyond a tumor location. Analogous motor deficits reported in pediatric patients with malignant glioma coincided with thinner bilateral motor cortices, providing intriguing evidence of a relationship between motor impairment and more distal morphological changes in glioma.[4] Currently unknown is how extensive structural changes are in the presence of a focally destructive GBM.

Functional imaging results provide evidence of the widespread impact of a tumor on the brain. Specifically, a broad range of neurological diseases, including GBM/HGG,[10–12] alter resting-state functional connectivity (rsFC), which characterizes the functional organization in the brain. Recent rsFC findings in GBM/HGG indicate prevalent distortions in the functional architecture, which extend beyond the focally malignant tissue and is bi-hemispheric in nature.[11–13] Notably, Stoecklein et al. found high-grade tumors associated with aberrant rsFC in the contralateral hemisphere.[14] Consequently, we hypothesized brain structural changes spread beyond the tumor site.

We first determined whether morphological changes in the brains of patients occurred in the contralesional hemisphere when compared to healthy controls (HC). We further examined whether these changes were prognostic of patient OS. Specifically, we estimated cortical thickness (CT) in the hemisphere contralateral to the tumor site of patients and compared it against HC. Then, we tested the prognostic significance of CT changes. Findings of widespread CT changes in the contralesional hemisphere supported the hypothesis of contralesional morphological changes in patients. Alterations in CT may potentially serve as a predictive biomarker to aid in decisions for the care of GBM/HGG patients.

Materials and Methods

Patients

We recruited GBM/HGG (World Health Organization [WHO] grade IV gliomas) patients retrospectively from Integrative Imaging Informatics for Cancer Research (I3CR) at Washington University in Saint Louis, Saint Louis, MO, USA, collected before March 2022 (since this is an ongoing study). Patient inclusion criteria stipulated newly diagnosed with a brain tumor, intracranial primary GBM/HGG (WHO grade IV gliomas) pathology and presurgical indication for structural MRI (T1-weighted [T1w], T2-weighted [T2w], fluid-attenuated inversion recovery [FLAIR], T1-postcontrast) as determined by the treating neurosurgeon. Pathology was also determined by a neuropathologist in all cases and was based on WHO criteria [15]. Exclusion criteria were younger than 18, prior surgery for a brain tumor, and bilateral tumor (since we focused on contralateral hemisphere morphometric changes). We also excluded patients still alive (until the last follow-up), those lost in follow-up, and patients with immediate postoperative complication-related mortality (if <30 days of postoperation). A further 65 patients failed Freesurfer segmentation resulting from a severe

Table 1. Demographics of the Study Sample and Clinical Information

Variables	Groups	
	HC	Patients (GBM/HGG)
Patients (*N*)	127	162 (RT = 69, LT = 93)
Sex		
Male	39	90
Female	88	72
Age (in years) (range)	61.9 (56–71)	61.3 (18–87)
Mean/median OS (range)	—	505/391.5 days (43–2048)
IDH1	—	
Mutated		2
Wild type		157
Missing		3
EGFR	—	
Positive		61
Negative		89
Missing		12
MGMT	—	
Methylated		55
Nonmethylated		99
Missing		8
Extent of resection	—	
Gross total		37
Near total		50
Subtotal		18
Biopsy		42
Missing		15
KPS	-	
>70%		125
<70		24
Missing		13

Abbreviations: CE, contrast-enhanced; EGRF, epidermal growth factor receptor; GBM/HGG, glioblastoma and high-grade glioma; HC, healthy control; IDH1, isocitrate dehydrogenase-1; KPS, Karnofsky performance score; LT, left hemispheric tumor; MGMT, methylguanine-DNA methyltransferase; OS, overall survival; RT, right hemispheric tumor.

topological defect or whose brains could not complete Freesurfer segmentation after a week (exceeded wall time which is 7 days and far above the median Freesurfer computation time for HC, which was about 9 h and that of patients 21 h for the computing system we used). We also excluded 23 patients with poor structural data quality following reviews by 3 researchers in the team. Further, cortical analysis on retained data included: *N* = 162, right tumor 69, and left tumor 93. Figure S1 illustrates, a CONSORT diagram, the details of patients' enrollment and exclusion.

For controls, we studied structural scans from 127 age-matched HC, publicly available Open Access Series of Imaging Studies[16] (OASIS3, https://www.oasis-brains.org). For the demographic of the study sample and clinical information, see Table 1. The Institutional Review Board of Washington University in St. Louis approved this study.

Segmentation

Freesurfer segmentation.—

We visually inspected T1w and T2w images to ensure brain structures were free of blurring, ringing, striping, ghosting, etc., caused by head motion during scanning. We used Freesurfer's recon-all option with both T1w and T2w images as input, in Freesurfer version 6.0 (http://surfer.nmr.mgh.harvard.edu/), to segment patients and HC.[17] Both the structural image: T1 weighted the magnetization prepared rapid acquisition (MP-RAGE), T2w fast spin echo, both with a voxel size of (1 mm)^3. Three raters (B.L, D.L.D., and G.T.V) reviewed tumor segmentation in both groups to ensure data quality. An example of a Freesurfer segmentation of the cortex in a patient and a healthy subject is shown in Figure S2.

Tumor segmentation.—

In order to segment a tumor and produce multiclass tumor segmentation maps of glioma, consisting of vasogenic edema, necrotic/nonenhancing core, and enhancing core, we pre-train a 3D CNN architecture [18] using postcontrast T1w, T2w, and FLAIR scans (for detail of the segmentation, see Supplementary Material). Figure S3 shows the distribution of tumor density, defined by contrast-enhanced (CE) T1w boundaries.

Post-Freesurfer Data Processing

We focused the post-Freesurfer analysis on 34 cortical parcels based on the Desikan–Killiany parcellation[19] and the mean of hemispheric CT. We also computed the lobar CT (mean of CT in frontal, parietal, temporal, occipital, and cingulate cortices, a total of 5 lobes defined by Freesurfer). Also, we included age, gender, and hemisphere as nuisance factors in multiple regression analysis and statistical analysis, when possible, as known to affect cortical structures to some extent.[20–22]

Multivariate regression model.—

Multiple regression models compared CT- between patients (GBM/HGG) and HC. The analysis focused on CT in 1 hemisphere per patient and similarly per HC cases. In patients, we focused on the hemisphere contralateral to the tumor. In HC, we randomly divided the cases, prior to multiple linear regression analysis, into 2 halves (left, *N* = 64; right, *N* = 63) and used 1 hemispheric CT per HC subject.

We executed model fitting with the R statistical language (R's linear model permutation function *lmp* from the l*mPerm* package[23]). Specifically, we estimated group difference using effect-coded group (ie, HC = –1, patients = 1) as a categorical variable in the regression analysis and CT as a function of

the group, age, sex, and hemisphere (Model 1: CT ~ group + age + sex + hemisphere) as CT may be confounded by age, sex, and hemisphere[5] (regardless of diseases). We assessed statistical significance with a permutation test, with a total number of iterations = 100,000, and used the *lmPerm* package from R.[23] Results were considered statistically significant with a *p*-value of the permutation (p) < 0.05.

We also reported the multiple comparison corrected *p*-values (ie, if original p × correction factor is ≤0.05, correction factor = 34 for parcelwise analysis and 5 for lobar analysis).

Statistical test of association between CT and overall survival.—
We assessed the association between CT and OS in patients using 3 methods. **Test 1**: Multivariate Cox proportional hazard model controlling for age, sex, and hemisphere. We also controlled for the extent of resection in multivariate Cox proportional hazard as it was found associated with survival.[24] **Test 2**: A test of median OS of low versus high CT patients. For this, patients were median divided into two groups: low CT (<median CT) and high CT. A Wilcoxon rank-sum test assessed the high and low CT groups' median OS. **Test 3**: A Kaplan–Meier analysis investigated the difference in survival between low and high CT groups.

Machine learning analysis.—
We assessed the feasibility of CT to classify patients into short-term (ST) versus long-term (LT) survival groups with respect to the reported median survival (14.6 months)[1] using random forest classifiers.[25] Random forests are ensemble methods composed of numerous decision trees. Each decision tree is trained on a random subset of the original data. This approach yields a set of "weak learners" whose individual outputs are not strongly correlated, and the final model output reflects the primary consensus of all the decision trees in the forest. The process of aggregating results from multiple weak learners into a final output generally leads to both higher accuracy and stronger generalization ability.[26] Further, a random forest can be categorized as an embedded feature selection method.[27] The strongest predictors of a given outcome are calculated by averaging the mean decrease in impurity for each feature for each tree. Model features included all CT measures, age, sex, and tumor hemisphere.

We trained the random forest with 10-fold nested stratified cross-validation. Nested cross-validation involves an "outer" partitioning of the data into k folds. Then within each individual outer fold, that data is again partitioned into k "inner" folds. Models are trained and optimized based on the given inner fold, and then the final result is based on testing the trained model on the held-out portion of the given outer fold. During training, model hyperparameters (aggregation method, number of learning cycles, learn rate, minimum leaf size, and maximum number of splits) were optimized with 200 iterations of Bayesian optimization. Within each forest, decision trees utilized a curvature test to construct a tree which minimizes the *p*-value of the chi-square tests of independence between each predictor and the response, and each pair of predictors and response.[28] The data within each fold was stratified based on length of survival, age, sex, and hemisphere. Reported outcome calculations reflected outer fold results.

Results

Study Samples

Table 1 lists the demographics of patients (GBM/HGG) and HC groups, and OS of the patients. Furthermore, the heatmap (Figure S3) illustrates the distribution of tumor density in the studied patient population as defined by CE T1w segmented boundaries.

Widespread Cortical Thinning in a Normal-Appearing Brain

We examined the difference in CT-between patients and HC at 3 different levels: hemispheric (ie, mean of CT over contralesional hemisphere), lobe label (mean of CT over brain lobes), and cortical parcels. Table 2 lists mean (±standard deviation) of measured CTs (ie, before correcting age, sex, and hemispheric effect) showing significant group differences. The *p*-value (permutation test) of significance in multiple linear regression models (Model 1). Table S1 presents the complete analysis that did not cross the $p < .05$ threshold in permutation resampling test. These results reveal the structural effects of focal gliomas, which extend to remote contralateral regions.

Mean cortical thickness in the contralesional hemisphere.—
The contralesional CT was significantly lower (Table 2, $p < .00034$, permutation test) in the patients than the HC group when comparing the mean CT of the contralateral hemispheric mean after regressing age, sex, and hemisphere. Figure S4 shows a distribution of mean CT in the contralateral hemisphere. This result indicates that a glioma causes a brain-wide CT thinning in a normal-appearing hemisphere contralateral to the glioma.

Mean cortical thickness over lobe in contralateral hemisphere.—
We then measured CT in 5 contralateral hemispheric lobes: frontal, parietal, temporal, occipital, and cingulate, using lobes defined by Freesurfer. After the permutation test, occipital ($p < 1.00E{-}16$), temporal ($p < .012$), and parietal ($p < 1.00E{-}16$) lobes were significantly thinner in patients compared with HC after regressing out the age, sex, and hemisphere (Table 2). Figure 1A shows difference in mean CT-between groups (GBM/HGG <HC) and the –log10 of the *p*-value of group difference (significant lobes only) in the multiple regression analysis (Figure 1B).

Mean cortical thickness over parcels in contralateral hemisphere.—
Patients had thinner cortices in 19 out of 34 cortical parcels (Tables 2 and S1 for complete analysis). CT results were from 6 frontal lobe parcels (eg, medial-orbitofrontal, paracentral, precentral), 3 parietal parcels (postcentral,

Table 2. Morphological Changes in the Brains of GBM/HGG Patients in the Contralesional Hemisphere Compared with HC

Cortical Structure	Mean CT ± SD (mm) (measured)		*p*-Value (permutation test)
	Patients (GBM/HGG)	Healthy controls	
Hemispheric CT	2.369 ± 0.138	2.413 ± 0.075	.00034*
Lobar CT			
Parietal	2.205 ± 0.161	2.275 ± 0.091	1.00E−16 *
Temporal	2.783 ± 0.161	2.827 ± 0.113	.012
Occipital	1.848 ± 0.110	1.923 ± 0.096	1.00E−16 *
Parcel CT			
Cuneus	1.779 ± 0.156	1.857 ± 0.135	1.00E−16*
Entorhinal	3.310 ± 0.334	3.464 ± 0.308	.0007*
Fusiform	2.601 ± 0.204	2.714 ± 0.107	1.00E−16 *
Inferior temporal	2.769 ± 0.17	2.732 ± 0.112	.0403
Lateral orbitofrontal	2.559 ± 0.184	2.522 ± 0.128	.0475
Lingual	1.939 ± 0.133	2.026 ± 0.107	1.00E−16 *
Medial orbitofrontal	2.256 ± 0.185	2.342 ± 0.142	1.00E−16 *
Middle temporal	2.834 ± 0.168	2.762 ± 0.118	1.00E−16 *
Parahippocampal	2.63 ± 0.274	2.733 ± 0.264	.0150
Paracentral	2.182 ± 0.266	2.381 ± 0.136	1.00E−16 *
Parsorbitalis	2.648 ± 0.234	2.590 ± 0.170	.0078
Parstriangularis	2.390 ± 0.196	2.352 ± 0.131	.0379
Pericalcarine	1.478 ± 0.116	1.613 ± 0.134	1.00E−16 *
Postcentral	1.942 ± 0.184	2.047 ± 0.106	1.00E−16 *
Posterior cingulate	2.304 ± 0.189	2.370 ± 0.130	.0014 *
Precentral	2.360 ± 0.226	2.485 ± 0.132	1.00E−16 *
Precuneus	2.221 ± 0.21	2.326 ± 0.104	1.00E−16 *
Superior parietal	2.079 ± 0.192	2.161 ± 0.105	.0004 *
Transverse temporal	2.105 ± 0.306	2.328 ± 0.200	1.00E−16 *

Abbreviations: CT, cortical thickness; GBM/HGG, glioblastoma and high-grade glioma; HC, healthy control.
Mean CT (±SD) of cortical hemisphere, lobes, and parcels of both patients and HC. The *p*-value represents group difference (GBM/HGG vs. HC) in multiple linear models (Model 1) of significant parcels (if $p < .05$ permutation test and $*p < .05$, Bonferroni correction on permutation resampled *p*-value).

precuneus, superior-parietal), 3 occipital parcels (cuneus, lingual, pericalcarine), 6 temporal parcels (entorhinal, fusiform, transverse-temporal), and 1 cingulate parcel (posterior-cingulate). However, cortical thickening appeared in 4 cortical parcels at the time of GBM/HGG diagnosis compared with HC. Two of these were in the frontal lobe (parsorbitalis, parstriangularis) and 2 from the temporal lobe (middle-temporal, inferior-temporal). Figure 1C showed the difference in CT between groups (GBM/HGG <HC and before correcting for age, sex and hemisphere) and Figure 1D, the –log10 of *p*-value of group difference (significant parcels only) in the multiple regression analysis (Model 1, after correcting the age and sex and hemisphere).

Association Between Brain-Morphological Change and Overall Survival

The relation between CT and OS was significant (if $p < .05$) on all 3 robust tests (Table 3) for assessments based on contralateral hemisphere, lobes, and parcels. Table S2 presents the complete analysis that did not cross 0.05 *p*-value threshold on all of 3 tests.

Relationship between mean contralateral hemispheric CT and overall survival.—

First, we tested the relation between contralateral hemispheric CT and OS using Cox proportional hazard model (controlling for age, sex, hemisphere, and extent of resection). There was a significant association between CT and OS (hazard ratio [HR]: 0.09, CI: 0.02, 0.44, $p = .003$). The Wilcoxon rank-sum (test 2) found that patients with low CT (<median CT) had significantly lower median OS (311 days) compared with high CT groups (525 days; Wilcoxon rank-sum, $W = 2120$, $p < .0001$; Table 3 and Figure 2A). Further, the Kaplan–Meier analysis (test 3) demonstrated a significant difference in survival between LOw and high CT groups ($Chi^2 = 13.42$, $p = .0003$; Table 3 and Figure 2B).

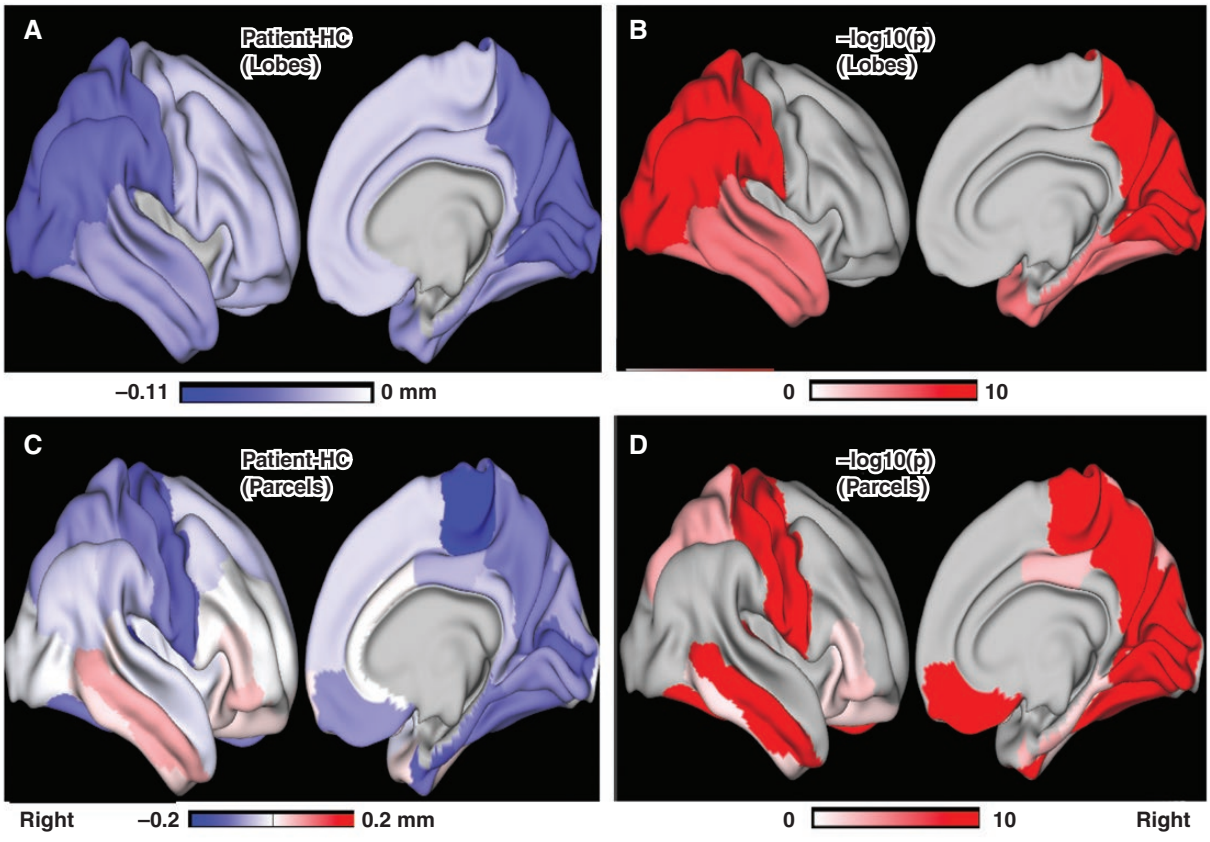

Figure 1. Visualization of differences in contralateral cortical thickness (CT; overlaid on human connectome project's surface mesh, for visualization purpose). The cortical map summarizes the parcel's CT. (A) The differences in lobar CT between groups (GBM/HGG-HC). (C) The differences in parcelwise CT between groups (GBM/HGG-HC). The negative value (blue) in both A and C represents the thinner cortex in patients compared to HC. (B and D) The plot of –log10 of the *p*-value of the group difference of lobar and parcel's CT, respectively (showing only the parcels survived in permutation test). GBM/HGG, glioblastoma and high-grade glioma; HC, healthy control.

Relationship between lobar CT and overall survival.— The prognostic value of lobar CT (mean of CT of frontal, parietal, temporal, occipital, and cingulate lobes defined by Freesurfer) in patients was also tested. First, we performed the Cox regression hazard proportional test of lobar CT. The effect was significant in lobes: frontal (HR: 0.20; CI: 0.05, 0.71; $p = .013$), parietal (HR: 0.11; CI: 0.03, 0.46; $p = .003$), and temporal (HR: 0.14; CI: 0.0.04, 0.50; $p = .003$; Table 3). Cingulate lobe remained insignificant in Cox tests (Table S1). Then, further analyses performed on parcels with tests 2 and 3 show significant Cox test results. All 3 lobes were found significant (all $p < .002$; Table 3). Please note that parietal and temporal lobes were the ones showing significant cortical thinning and frontal was trending to significant (HC vs. GBM/HGG).

Relationship between parcel's CT and overall survival.— We further investigated the association between cortical changes in the contralesional parcels and OS in all 3 tests. Significant results in the 11 parcels for the 3 tests (Table 3) supported the significant association of CT and OS (Table 3). Table S2 presents the analytics.

Classification using machine learning.— Modern machine learning analytics yield stronger generalizations by aggregating results from multiple features into a final output, regardless of whether features are in a traditional statistical analysis. Thus, we used CT in machine learning analytics to examine the hypothesis that CT provides biomarkers for the duration of survival in patients. Figure 3 displays the results of using Random forest to classify patients as ST versus LT survivors. Patients were categorized based on the median survival of 14.6 months reported in the literature.[1] The model was able to classify patients correctly with 83.3% accuracy (Figure 3A). The model classified ST survivors with higher accuracy (89.7%) than LT survivors (76%). Figure 3B shows the top 10 strongest features used by the decision trees to classify the patients as ST versus LT survivors. Age was the only demographic variable identified as a strong predictor. On the parcel level, superior temporal, precuneus, inferior parietal, paracentral, superior frontal, and caudal middle frontal were strong predictors. At the lobe level, the frontal and occipital lobes were strong predictors. Global CT (mean thickness) was also a strong predictor.

Table 3. Survival Analysis

Cortical structure	Test 1, Multivariate Cox		Test 2, Wilcoxon Rank-Sum Test			Test 3, KM	
	HR (CI: L, U)	*p*	Median OS (Low, High CT) days	*W*	*p*	Chi^2	*p*
Hemispheric CT	0.09(0.02, 0.44)	.003*	311,525	2120	.0001*	13.42	.0003*
Lobar CT							
Frontal	0.20(0.05 0.71)	.013	314,525	2221	.0004*	10.7	.001*
Parietal	0.11(0.03, 0.46)	.003*	289,527	1879	2.7E–5*	21.3	3.9E–6*
Temporal	0.14(0.04, 0.50)	.003*	311,527	2078	5.6E–5*	10.1	.002*
Parcel CT							
Fusiform	0.15(0.05, 0.48)	.0007*	334,525	2163	.0002*	12.23	.0005*
Inferior parietal	0.17(0.05, 0.56)	.004	321,508	2284	.0008*	10.50	.0012*
Lateral orbitofrontal	0.24(0.08, 0.75)	.014	324,530	2221	.0004*	9.43	.0021
Paracentral	0.32(0.14, 0.75)	.008	324,480	2171	.0002*	13.57	.0002*
Parsopercularis	0.23(0.08, 0.63)	.005	312,522	2259	.0006*	9.21	.0024
Precuneus	0.26(0.09, 0.73)	.010	314,530	1970	1.1E–5*	18.81	1.4E–5*
Rostral middlefrontal	0.27(0.10, 0.73)	.010	312,525	2148	.0002*	16.5	4.8E–5*
Superior frontal	0.28 (0.09, 0.82)	.020	334,491	2367	.0002*	9.16	.002
Superior-parietal	0.34 (0.13, 0.88)	.011	334,472	2344	.0018	10.83	.0009*
Superior temporal	0.34 (0.13, 0.88)	.026	314,525	2188	.0002*	14.38	.0001*
Supramarginal	0.26 (0.08, 0.83)	.022	314,472	2250	.00057*	10.39	.0013*

Abbreviations: CT, cortical thickness; HR, hazard ratio; OS, overall survival.
Test 1: Multivariate Cox proportional hazards model was performed (with age, sex and hemisphere). Test 2: Wilcoxon rank-sum test of median overall survival of low versus high cortical thickness patients (WRS). Test 3: Kaplan–Meier test of survival difference (KM; *$p < .05$, Bonferroni correction).

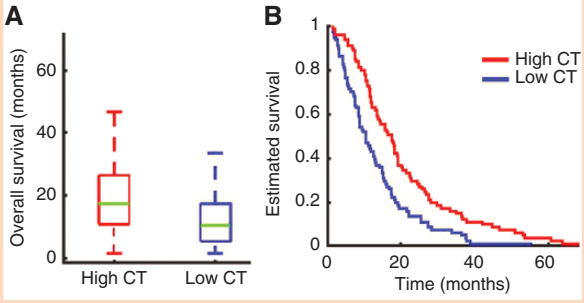

Figure 2. (A) Overall survival in patients with low cortical thickness (CT) (<median CT) differed significantly from overall survival in patients with high CT (>median CT; Wilcoxon rank-sum, $W = 2120$, $p < .0001$). (B) Kaplan–Meier survival analysis comparing overall survival in low CT patients and high CT patients (Chi^2=13.42, $p = .0003$).

Discussion

We found thinning of contralesional CT in patients. This was a novel clinical finding. These results demonstrate GBM/HGG patients already had diffuse changes in brain morphology at the time of diagnosis. Predictive of OS were morphologic changes in the hemisphere, lobes, and parcels contralateral to the GBM/HGG. We determined the feasibility of using measurements of CT to classify patients into ST and LT survival groups with respect to reported median survival with high accuracy, using machine learning analytics. The findings also revealed widespread structural alterations associated with focal glioma, identifiable with noninvasive imaging to obtain potentially important and readily accessible prognostic biomarkers.

Widespread Reduction in Cortical Thickness in Patients

The central finding was widespread cortical thinning in patients compared with HC (Figure 1 and Table 2) at the time of diagnosis. CT was present at the hemispheric level, several lobes (parietal, temporal, and occipital), and selected cortical parcels. Cortical areas showing significant thinning involved regions associated with higher-order multisensory and cognitive processing (eg, precuneus, superior-parietal), motor processing (eg, paracentral), and sensory functions (eg, somatosensory: postcentral auditory: transverse-temporal; occipital and higher-order visual areas, pericalcarine, cuneus, lingual). Four cortical parcels were significantly thicker in GBM/HGG, as previously reported.[29]

Changes in CT are strongly correlated with the presence of GBM/HGG. Several possible hypotheses possibly manifest a causal mechanism for the observed morphological changes. (1) An "oncologic-metabolic hypothesis" might involve a rapidly growing tumor that parasitizes nutrients,

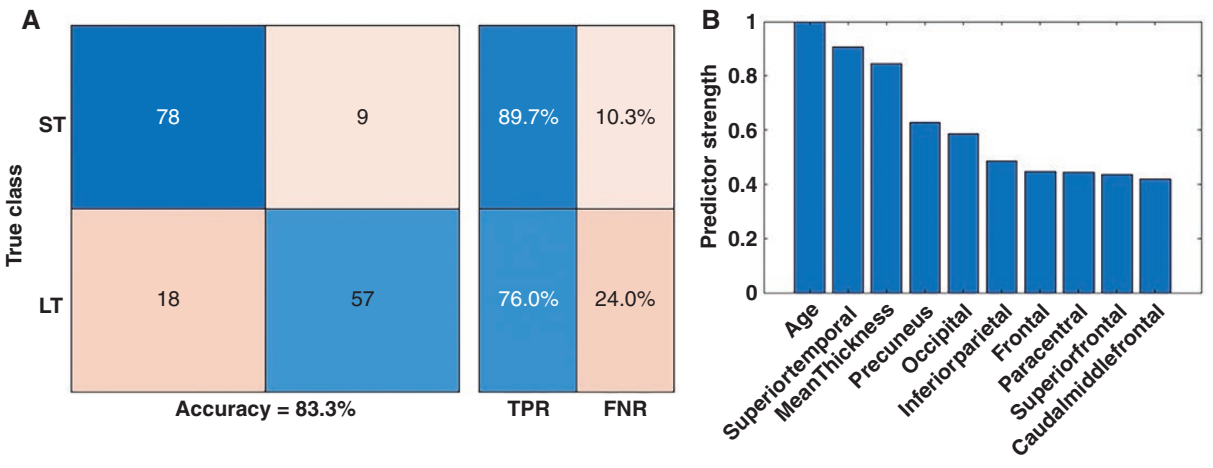

Figure 3. (A) Nested cross-validation classification accuracy of random forest models for classifying patients as short-term (ST) versus Long-term (LT) survivors based on median survival. The overall accuracy of the model was 83.3%. The model correctly classified ST with 89.7% accuracy and LT with 76% accuracy. (B) The top 10 strongest features used by the random forest for survival classification based on embedded feature selection. The strongest features included age and various brain regions at different scales.

resulting in cortical atrophy from depriving more metabolically and synthetically active regions of the brain. (2) A "functional hypothesis" might involve a locally destructive tumor, which asserts distant effects through altered connectivity and/or synaptic homeostasis. These thereby reduce inputs and subsequent diminution to remote cortical sites. (3) An intriguing third option is the "predisposition hypothesis." Specifically, cortical changes noted at the time of GBM/HGG diagnosis precede oncogenesis and rather reflect brain health in a patient predisposed to developing a tumor. Further work will be required to better define a mechanistic underpinning for the observed changes in CT.

Cortical Thickness: A Potential Biomarker of Survival

Contralateral CT showed significant group differences in patients compared with HC and in relation to OS in all 3 tests. We also found an association between OS and CT in the parietal and temporal lobes, which also showed significant group differences in CT (GBM/HGG vs. HC). CT in several parcels showed similar group differences. Important clinically, patients with thinner cortex had shorter survivals. A machine learning analysis of CT predicted patient survival, a finding toward the development of quantitative prognostic markers to inform pretreatment planning, patient counseling, and improve outcomes.

The neurobiology of widespread cortical thinning particularly to GBM/HGG remains unclear. However, conceivably CT marks disease severity (both metabolic and/or functional [4,30,31]). Contralateral cortical parcels and lobes serve multiple higher-order multisensory, cognitive, and motor and sensor processing functions. Motor deficits commonly reported in patients with malignant glioma correlated with thinner motor cortices.[4] Most patients with GBM/HGG are cognitively impaired before initiating any treatment.[6,7] Although speculative, neurocognitive and motor deficits in patients with other types of brain tumors, prior to any treatment, may be related to CT in combination with other factors.[32] However, widespread functional network anomalies [11–14,33] and contralateral cortical gray matter changes may not be explained merely by the tumor location and affected local damage. The contralateral hemispheric changes in CT in patients with GBM/HGG indicate a need to widen searches for brain-morphological disruption beyond tumor locations.

Limitations

Many patients, especially with larger tumors, failed to achieve Freesurfer segmentation, possibly because of technical issues with Freesurfer. Consequently, usable samples had a relatively small tumor size. Where possible, the analysis accounted the effects of the hemisphere, patient sex, age, and resection status. Other known factors affecting prognosis in GBM/HGG patients were tumor volume, IDH1 status, epidermal growth factor receptor, methylguanine-DNA methyltransferase promoter methylation promoter methylation, and other clinical and personal characteristics. However, the Cox model analysis failed to operate with all of the multiple features. Although we used machine learning analytics, which aggregate results from multiple features, regardless of statistical significance of features, there remain issues regarding reproducibility and generalizability of results. Future studies will require more patients with high-quality structural scans to confirm and expand current findings. Furthermore, there is a pressing need for future studies of multivariate biomarker of OS in patients including variables such as rsFC, radiomic features, and clinical and personal characteristics.

There are several methods and experimental approaches that can potentially better inform these anatomical findings. Animal brain tumor models will be an important tool to

identify differences in contralesional metabolism, such as mitochondrial density, gene expression, tissue cytoarchitecture, and proteonimcs. From a system neuroscience perspective, rsFC is an important metabolic measure of synaptic homeostasis that may inform changes in cortico-cortical interactions associated with this cortical thinning phenomenon.

Conclusions

At the time of diagnosis, patients with GBM/HGG have multiple regions with cortical thinning in the hemisphere contralateral to the tumor. Further, the hemisphere CT, and a subset of these morphological changes (ie, cortical thinning in lobes and parcels) were strongly predictive of survival in patients. These findings support the widespread impact of GBM/HGG on the brain and provide a foundation for a potentially readily accessible prognostic radiomic biomarker.

Supplementary material

Supplementary material is available online at *Neuro-Oncology* (http://neuro-oncology.oxfordjournals.org/).

Keywords

biomarker of GBM and HGG | brain tumor | cortical thickness | glioblastoma and high-grade glioma | overall survival.

Funding

This research was supported by the National Cancer Institute of the National Institute for Health via grant R01CA203861.

Acknowledgments

We would like to thank Dr. Leuthardt's, Dr. Burton's, Dr. Brunner's lab team for helpful input and discussions regarding the data analysis of this study.

Authorship

B.L. and E.C.L. designed the study; B.L., M.O, D.S.M., and J.S.S. and assembled the data; B.L. and D.D. performed preprocessing (Freesurfer segmentation) of the data; B.L. and P.L. performed the post-data analysis; B.L., G.T., K.P., and J.S.S. performed tumor segmentation and QC; B.L. prepared the first draft; H.B., E.C.L., D.D., J.J.L., and C.D.H. review and edited the first draft. All authors critically reviewed and edited the manuscript.

Conflict of interest

E.C.L. has equity in Neurolutions, Inner Cosmos. E.C.L., D.S.M., and C.D.H. have equity in Sora Neuroscience. E.C.L, J.J.L., and J.S.S. have patent interests licensed to Sora Neuroscience. D.S.M. has equity in Radiologics, Inc. Washington University has equity in Neurolutions. B.L and E.C.L. have filed a provisional patent on the techniques described in this manuscript. All other authors declared that they had no conflicts of interest to their authorship or the publication of this article.

Data availability

Tumor data will be made available upon request to E.C.L.

References

1. Stupp R, Hegi ME, Mason WP, et al. Effects of radiotherapy with concomitant and adjuvant temozolomide versus radiotherapy alone on survival in glioblastoma in a randomised phase III study: 5-year analysis of the EORTC-NCIC trial. *Lancet Oncol.* 2009;10(5):459–466.
2. Blumen HM, Schwartz E, Allali G, et al. Cortical thickness, volume, and surface area in the motoric cognitive risk syndrome. *J Alzheimers Dis.* 2021;81(2):651–665.
3. Julkunen V, Niskanen E, Koikkalainen J, et al. Differences in cortical thickness in healthy controls, subjects with mild cognitive impairment, and Alzheimer's disease patients: a longitudinal study. *J Alzheimers Dis.* 2010;21(4):1141–1151.
4. Szulc-Lerch KU, Timmons BW, Bouffet E, et al. Repairing the brain with physical exercise: cortical thickness and brain volume increases in long-term pediatric brain tumor survivors in response to a structured exercise intervention. *NeuroImage Clin.* 2018;18:972–985.
5. Plessen KJ, Hugdahl K, Bansal R, Hao X, Peterson BS. Sex, age, and cognitive correlates of asymmetries in thickness of the cortical mantle across the life span. *J Neurosci.* 2014;34(18):6294–6302.
6. Taphoorn MJB, Klein M. Cognitive deficits in adult patients with brain tumours. *Lancet Neurol.* 2004;3(3):159–168.
7. Van Kessel E, Emons MAC, Wajer IH, et al. Tumor-related neurocognitive dysfunction in patients with diffuse glioma: a retrospective cohort study prior to antitumor treatment. *Neuro-Oncol Pract.* 2019;6(6):463–472.
8. Klein M. Lesion momentum as explanation for preoperative neurocognitive function in patients with malignant glioma. *Neuro-Oncology.* 2016;18(12):1595–1596.
9. Noll KR, Sullaway C, Ziu M, Weinberg JS, Wefel JS. Relationships between tumor grade and neurocognitive functioning in patients with glioma of the left temporal lobe prior to surgical resection. *Neuro-Oncology.* 2014;17(4):580–587.
10. Lamichhane B, Daniel AGS, Lee JJ, et al. Machine learning analytics of resting-state functional connectivity predicts survival outcomes of glioblastoma multiforme patients. *Front Neurol.* 2021;12(February):1–10.
11. Manan HA, Franz EA, Yahya N. Functional connectivity changes in patients with brain tumours—a systematic review on resting state-fMRI. *Neurol Psychiatry Brain Res.* 2020;36(July):73–82.

12. Catalino MP, Yao S, Green DL, et al. Mapping cognitive and emotional networks in neurosurgical patients using resting-state functional magnetic resonance imaging. *Neurosurg Focus*. 2020;48(2):E9E9.
13. Maesawa S, Bagarinao E, Fujii M, et al. Evaluation of resting state networks in patients with gliomas: connectivity changes in the unaffected side and its relation to cognitive function. *PLoS One*. 2015;10(2):e011807 21–e01180713.
14. Stoecklein VM, Stoecklein S, Galiè F, et al. Resting-state fMRI detects alterations in whole brain connectivity related to tumor biology in glioma patients. *Neuro-Oncology*. 2020;22(9):1388–1398.
15. Louis DN, Perry A, Wesseling P, et al. The 2021 WHO classification of tumors of the central nervous system: a summary. *Neuro-Oncology*. 2021;23(8):1231–1251.
16. LaMontagne PJ, Benzinger TLS, Morris JC, et al. OASIS-3: longitudinal neuroimaging, clinical, and cognitive dataset for normal aging and Alzheimer disease. *medRxiv*. 2019. doi:10.1101/2019.12.13.19014902
17. Fischl B, Dale AM. Measuring the thickness of the human cerebral cortex from magnetic resonance images. *Proc Natl Acad Sci*. 2000;97(20):11050 LP–11011055.
18. Isensee F, Kickingereder P, Wick W, Bendszus M, Maier-Hein KH. Brain tumor segmentation and radiomics survival prediction: contribution to the BraTS 2017 challenge. In: Crimi A, Bakas S, Kuijf H, Menze B, Reyes M, eds. *International MICCAI Brainlesion Workshop*. Springer; 2017:287–297.
19. Desikan RS, Ségonne F, Fischl B, et al. An automated labeling system for subdividing the human cerebral cortex on MRI scans into gyral based regions of interest. *Neuroimage*. 2006;31(3):968–980.
20. Kinno R, Muragaki Y, Maruyama T, et al. Differential effects of a left frontal glioma on the cortical thickness and complexity of both hemispheres. *Cereb Cortex Commun*. 2020;1(1):1–11.
21. Salat DH, Buckner RL, Snyder AZ, et al. Thinning of the cerebral cortex in aging. *Cereb Cortex*. 2004;14(7):721–730.
22. Toga AW, Thompson PM. Mapping brain asymmetry. *Nat Rev Neurosci*. 2003;4(1):37–48.
23. Wheeler RE. *lmPerm. R Proj Stat Comput* https://cran.r-project.org/web/packages/lmPerm/lmPerm.pdf. 2010.
24. Han Q, Liang H, Cheng P, Yang H, Zhao P. Gross total vs. subtotal resection on survival outcomes in elderly patients with high-grade glioma: a systematic review and meta-analysis. *Front Oncol*. 2020;10:151.
25. Breiman L. Random forests. *Mach Learn*. 2001;45(1):5–32.
26. Zhou Z-H. Ensemble learning. In: Li SZ, Jain A, eds. *Encyclopedia of Biometrics*. Boston, MA: Springer, 2009.
27. Saeys Y, Inza I, Larrañaga P. A review of feature selection techniques in bioinformatics. *Bioinformatics*. 2007;23(19):2507–2517.
28. Loh W-Y. *Regression Trees with Unbiased Variable Selection and Interaction Detection*. 2002.
29. McIntosh EC, Jacobson A, Kemmotsu N, et al. Does medial temporal lobe thickness mediate the association between risk factor burden and memory performance in middle-aged or older adults with metabolic syndrome? *Neurosci Lett*. 2017;636:225–232.
30. de la Cruz F, Schumann A, Suttkus S, et al. Cortical thinning and associated connectivity changes in patients with anorexia nervosa. *Transl Psychiatry*. 2021;11(1):95.
31. Shivamurthy VKN, Tahari AK, Marcus C, Subramaniam RM. Brain FDG PET and the diagnosis of dementia. *AJR Am J Roentgenol*. 2015;204(1):W76–W85.
32. van Kessel E, Emons MAC, Wajer IH, et al. Tumor-related neurocognitive dysfunction in patients with diffuse glioma: a retrospective cohort study prior to antitumor treatment. *Neuro-Oncol Pract*. 2019;6(6):463–472.
33. Tucha O, Ph D, Smely C, et al. Cognitive deficits before treatment among patients with brain tumors. *Neurosurgery*. 2000s47(2):324–333.